

Changes in the flow of Atlantic water into the Arctic Ocean since the last deglaciation: Evidence from the northern Svalbard continental margin, 80°N

Marta A. Ślubowska,^{1,2} Nalân Koç,³ Tine L. Rasmussen,² and Dorthe Klitgaard-Kristensen³

Received 3 February 2005; revised 9 August 2005; accepted 29 August 2005; published 23 November 2005.

[1] The Svalbard archipelago is located in the high Arctic (76°–80°N) within the northernmost reach of the West Spitsbergen Current, which is the continuation of the North Atlantic Current. In this specific setting close to the Polar Front, even small variations in the current system are expected to give large and distinct signals in paleoceanographic parameters. Thus the Svalbard area is ideal for monitoring the past history of the inflow of Atlantic water to the Arctic Ocean. We have studied sediment core NP94-51 taken outside the mouth of the Hinlopen Strait on the northern Svalbard shelf. The paleoceanographic development of the last deglaciation and the Holocene has been reconstructed using benthic and planktonic foraminifera, oxygen isotopes, and ice-rafted detritus. The results show that the first strong subsurface inflow of Atlantic water to the Arctic Ocean after the Last Glacial Maximum commenced at 12.6 ¹⁴C kyr B.P. (circa 15,000 calendar (cal) years B.P.) during the Bølling-Allerød interstadial. During the Younger Dryas, polar conditions prevailed at the surface with extensive sea ice cover, and the inflow of Atlantic-derived water was generally diminished. The inflow of more saline, but still cold Atlantic water was relatively strong during the early Holocene and caused intensified seasonal biological productivity. The Atlantic water inflow declined gradually during the mid-Holocene. Between 4500 and 1100 cal years B.P. the inflow was very weak, and the bottom waters over the northern Svalbard margin were cold and of lower salinity. During the last ~1000 years, climatic conditions improved such that the subsurface inflow of Atlantic-derived water increased. However, the surface waters were still cold.

Citation: Ślubowska, M. A., N. Koç, T. L. Rasmussen, and D. Klitgaard-Kristensen (2005), Changes in the flow of Atlantic water into the Arctic Ocean since the last deglaciation: Evidence from the northern Svalbard continental margin, 80°N, *Paleoceanography*, 20, PA4014, doi:10.1029/2005PA001141.

1. Introduction

[2] The Arctic climate at present is showing signs of rapid change. Satellite data show that sea ice cover over the Arctic Ocean is decreasing, on average by 2–3% per decade [Chapman and Walsh, 1993; Johannessen *et al.*, 1999; Comiso, 2002; Johannessen *et al.*, 2004; Comiso and Parkinson, 2004]. The Arctic perennial ice cover has declined as much as 9.2% from 1978 to 2000 [Comiso, 2002]. Over the past two decades surface temperature at latitudes higher than 60°N has increased at an average rate of 0.5°C per decade [Comiso, 2003]. Snow cover has diminished at a rate of 2.6% per decade [Armstrong and Brodzik, 2001] and permafrost has decreased [Tarnocai, 1999]. Satellite data show expansion of the melt regions in the large land ice masses and glaciers in the Northern Hemisphere [Comiso and Parkinson, 2004] contributing to the sea level rise. The cold halocline layer insulating the ice

from the warm Atlantic water below has thinned and disappeared in some areas [Steele and Boyd, 1998]. Oceanographic data indicate warming and increased extent of Atlantic-derived waters in the Arctic Ocean at 200–900 m depth, which seems consistent with greater inflow of Atlantic waters forced by change to the positive mode of the North Atlantic Oscillation/Arctic Oscillation (NAO/AO) [Quadfasel *et al.*, 1993; Grotefendt *et al.*, 1998; Serreze *et al.*, 2000]. Between 1997 and 2000, the heat flow in the West Spitsbergen Current (WSC) increased from 30 to 40 TW as a result of both increased speed and temperature [Schauer *et al.*, 2004].

[3] The West Spitsbergen Current (WSC), especially its narrow slope-confined warm core, is the major pathway for warm and saline Atlantic water to enter the Arctic Ocean [Aagaard and Greisman, 1975; Saloranta and Haugan, 2001]. The heat transport has a significant influence on the hydrographic conditions in the Arctic Ocean and on water mass modifications in the Nordic Seas, and to some extent the overflow into the North Atlantic. However, the geological history of the inflow of Atlantic water to the Arctic Ocean via the Fram Strait and along the western and northern Svalbard shelf is relatively poorly constrained; even more so for the last deglaciation and the Holocene. This is mainly due to the lack of high-resolution data, well

¹The University Centre in Svalbard, Longyearbyen, Norway.

²Department of Geology, University of Tromsø, Tromsø, Norway.

³Norwegian Polar Institute, Polar Environmental Centre, Tromsø, Norway.

Table 1. Cores Studied, Coring Device Used, Their Positions, Water Depth, and Length

Core	Type of Core	Position		Water depth, m	Length, cm
		Latitude, N	Longitude, E		
NP94-51BC1	box	80°21.403	16°18.125	398	40
NP94-51GC1	gravity	80°21.411	16°17.942	399	115
NP94-51SC2	Selcore	80°21.469	16°17.945	400	713

dated records and difficulties in accessing the area because of extensive sea ice cover. The few available studies for this time period have mainly focused their investigations on the eastern Barents Sea and the Barents slope [Polyak and Mikhailov, 1996; Lubinski *et al.*, 1996; Hald and Aspeli, 1997; Hald *et al.*, 1999; Duplessy *et al.*, 2001; Lubinski *et al.*, 2001; Sarthein *et al.*, 2003] or the western Svalbard fjords [Hald *et al.*, 2001, 2004]. Only one record covering the last deglaciation has been available from the northern Svalbard margin [Koç *et al.*, 2002].

[4] To assess and elucidate both the timing and variability of the Atlantic water inflow to the Arctic Ocean since the last glacial period, we studied three sediment cores (compiled to one record) (Table 1), retrieved from a high

accumulation area at the mouth of the northern Hinlopen Trough at the northern Svalbard continental margin at 80°N (Figure 1). We expect the study site to be highly sensitive to any changes in the advection of the Atlantic water since it is located within the northernmost reach of the West Spitsbergen Current.

2. Physical Setting and Oceanography

2.1. Physical Setting

[5] The Svalbard archipelago is situated in the high Arctic between 76° and 81°N (Figure 1). At present it is 60% covered by glaciers and ice caps. In spite of its high Arctic setting, its climate is modified by the WSC, the northern-

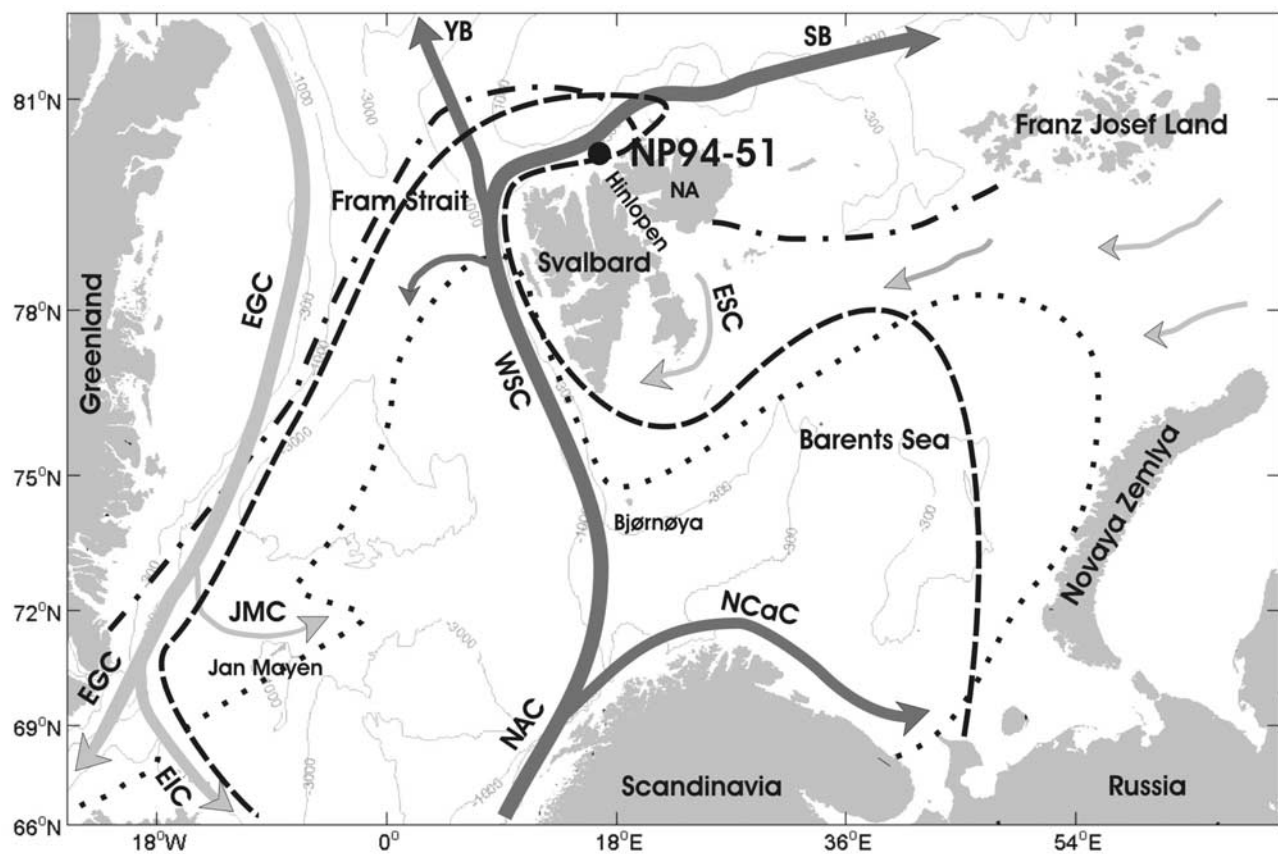


Figure 1. Location of the study site NP94-51 together with main current systems in the region, Polar Front (dashed line), average winter (dotted line) and summer (dashed-dotted line) sea ice margin [after Vinje, 1977]. Dark grey currents indicate warm currents, whereas light grey currents indicate cold currents. Abbreviations are NAC, North Atlantic Current; WSC, West Spitsbergen Current; ESC, East Spitsbergen Current; EGC, East Greenland Current; NCaC, North Cape Current; EIC, East Iceland Current; JMC, Jan Mayen Current; SB, Svalbard Branch; YB, Yermak Branch; and NA, Nordaustlandet.

most extension of the North Atlantic Current. The winter mean annual temperature on the western coast is -12°C and the mean July temperature is 5°C [Hisdal, 1998]. The largest island of the archipelago, Spitsbergen, is separated from Nordaustlandet Island by a ~ 170 km long strait, the Hinlopen Strait. The strong tidal stream in this strait runs along the axis of the strait northward with the rising tide and southward with the falling tide. From the northern mouth of the strait a deep trough (~ 400 m), called the Hinlopen Trough, extends northward to the shelf edge (Figure 1).

2.2. Oceanography

[6] The Nordic Seas and thus the North Atlantic and the Arctic Ocean are connected together via the Fram Strait, which is the only deep strait (2600 m) situated between Spitsbergen and Greenland allowing for the exchange of heat and fresh water (Figure 1). In the Fram Strait two main currents meet: the warm and saline WSC, which forms the continuation of the North Atlantic Current (NAC), and the East Greenland Current (EGC) passing southward. The EGC is the largest of export paths of sea ice from the Arctic Ocean via the Fram Strait [Saloranta and Haugan, 2001]. The WSC, which transports Atlantic water, Atlantic Intermediate water and Norwegian Sea Deep Water, is considered to be the main source of the warm and saline water of Atlantic origin to the Arctic [Aagaard and Greisman, 1975]. The WSC submerges in the Fram Strait at about 78°N and forms the Atlantic Layer (AL: temperature 0° – 2°C and salinity of 34.7–35‰) [e.g., Aagaard and Carmack, 1989], which moves into the Arctic Ocean along the northern continental slope of Svalbard. Rudels [1987] and Aagaard and Carmack [1989] provided estimates of the inflow of the Atlantic water through the Fram Strait to be about 1 Sv from which 0.2 Sv (the upper 100 m) is transformed into the colder and fresher waters in the polar mixed layer north of Svalbard [Rudels et al., 1999]. More recent studies [Grotefendt et al., 1998; Dickson et al., 2000], however, show that estimates of the volume of transport of the Atlantic water (AW) into the Arctic basin are still not well constrained and require further studies. Several studies have shown that the currents follow the bathymetry of the seafloor [Rudels, 1987; Pfirman et al., 1994] and that the topography intensifies the tidal force [Kowalik and Proshutinsky, 1995]. This behavior applies also to the West Spitsbergen Current, which flows over the upper continental slope and at $\sim 79.5^{\circ}\text{N}$ the slope isobaths separate and the WSC splits into two branches. One branch, the “Yermak branch,” flows northwest toward the Yermak Plateau losing its Atlantic water character rapidly [Manley, 1995]. The other branch, the “Svalbard branch” [Manley, 1995], seems to supply the major portion of the Atlantic water, in the form of the Atlantic Layer, into the Arctic Ocean [Aagaard et al., 1987; Manley, 1995; Rudels et al., 1999]. The Atlantic Layer is located between 100–200 and 600–800 m water depth with a main core of the layer having temperatures 3° – 4.5°C at 100–400 m water depth [Pfirman et al., 1994].

[7] At the study area six CTD profiles (Figures 2a–2c) were taken during the summer 1994 [Solheim and Forsberg,

1996]. We observe the Atlantic Layer at a water depth of 25 to 600 m with a maximum temperature of 3.5° – 4.0°C (Figure 2a) and salinity of 34.3–34.9‰ (Figure 2b) at 80–500 m.

3. Material and Methods

[8] We present results from sediment cores NP94-51SC2, NP94-51GC1 and NP94-51BC1 (Table 1). They were retrieved from the northern Svalbard continental margin from 400 m water depth during the 1994 Norwegian Polar Institute cruise onboard the R/V *Lance* [Solheim and Forsberg, 1996] (Figure 1). Acoustic surveys were used to identify undisturbed, soft and acoustically transparent quaternary sediment packages for selecting the core sites.

[9] On the basis of the AMS ^{14}C chronology we have compiled the three cores (Table 1) into a continuous record with a good overlap, and hereafter referred to as NP94-51. Methods and results from the deglacial period (514–713 cm down core in NP94-51SC2) were previously published by Koç et al. [2002]. The data are included here for comparison with the Holocene climate development. The present study focuses on the Holocene interval from the hitherto uninvestigated upper part of the NP94-51SC2 core (30–513 cm). For the most recent sediments the gravity core NP94-51GC1 and the box core NP94-51BC1 were analyzed as well (Table 1).

[10] The Holocene interval of all three cores is sampled for benthic and planktonic foraminifera at 5 cm intervals and the foraminifera were counted on the >100 μm fraction. The interval covering the last deglaciation was sampled previously at 1 cm intervals and the foraminifera were counted on the >125 μm fraction [Koç et al., 2002]. The difference in the two sieve fractions may affect the small sized species occurring in the Arctic. However, at present we regard this as a minor problem for the inferences on the paleoenvironment in this study. The reason for using different sieve fractions is discussed by Knudsen and Austin [1996]. Approximately 300 benthic foraminifera have been counted in each sample and identified to species level. Owing to the very low abundance of planktonic foraminifera in the samples, all specimens were counted and identified to species level. However, the numbers of specimens were too low for quantitative analysis and therefore only the total abundance of planktonic foraminifera is presented. Agglutinated foraminifera were generally very rare, except for the top of the box core. The nearly complete absence of agglutinated foraminifera down core indicates a low preservation potential of the agglutinated fauna. The concentration of foraminifera was calculated as number of specimens per gram dry bulk sediment. The most common species had well preserved tests and there were no indications of significant transportation or dissolution.

[11] The mineral grains were counted in the >100 μm fraction in the Holocene part of the core, whereas the deglaciation part was counted on the >125 μm fraction [Koç et al., 2002]. Approximately 300 grains were counted in each sample. The concentration of the IRD has been calculated as number of grains per gram dry sediment.

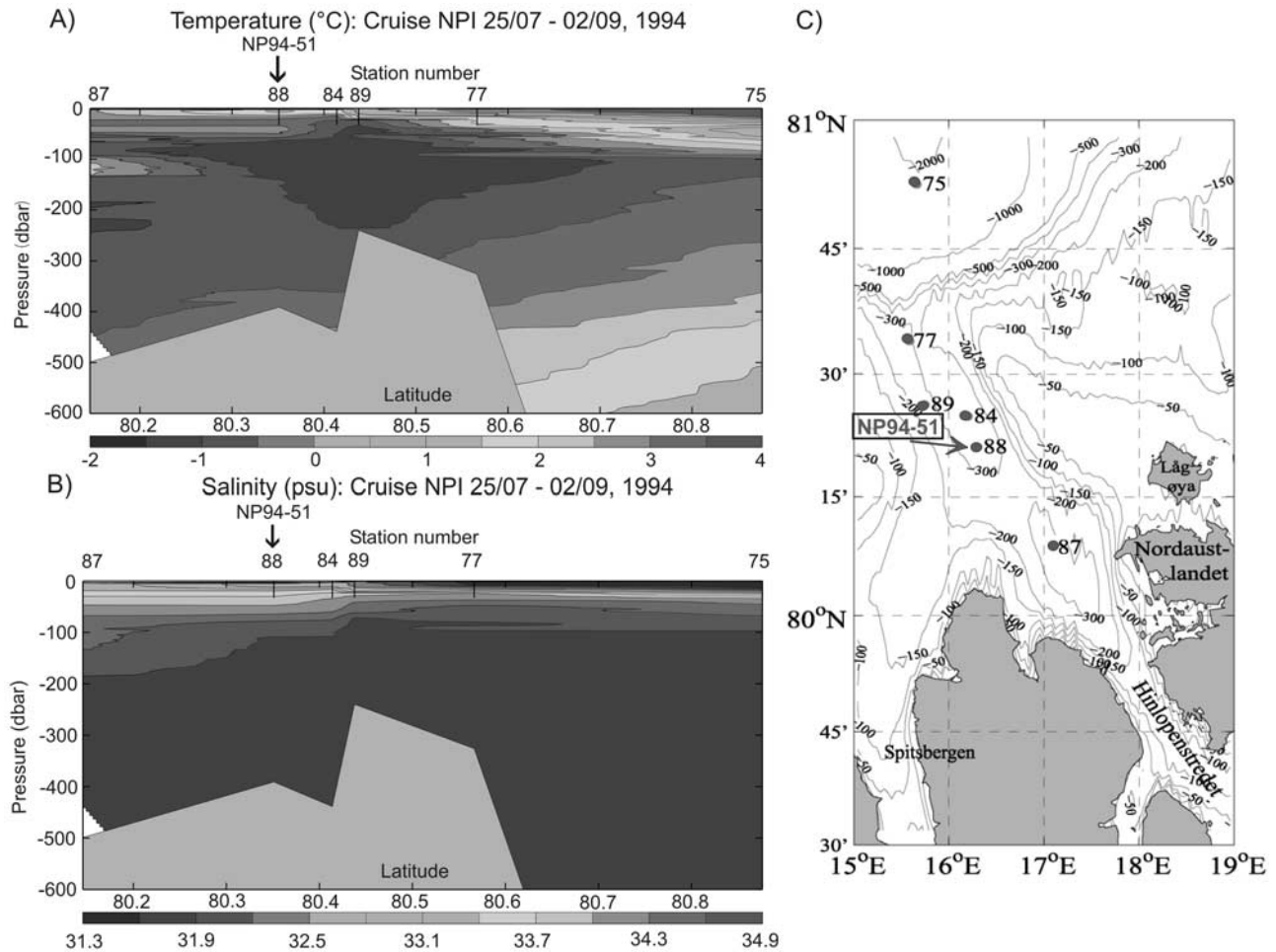


Figure 2. (a) Contours of potential temperature and (b) contours of potential salinity derived from (c) section taken at the northern Svalbard continental margin close to the Hinlopen Strait. Arrow in Figures 2a and 2b indicates the position of the NP94-51 core. The conductivity-temperature-depth (CTD) station measurements, marked by dots on the map (Figure 2c), were taken on 23–29 of August 1994. The sections are shown from S to N, and contour intervals are 1°C for temperature (Figure 2a) and 0.6‰ for salinity (Figure 2b). The CTD station 88 (Figure 2c) was taken at the same location as the NP94-51 core ($80^{\circ}21.40\text{N}$ and $16^{\circ}17.60\text{E}$). See color version of this figure at back of this issue.

[12] Oxygen isotope measurements were performed at the Geological Mass Spectrometer (GMS) laboratory at the University of Bergen, Norway. The Finnigan MAT 251 and 252 mass spectrometers both equipped with automatic preparation lines were used. The benthic foraminifera *Melonis barleeanum* were analyzed at 5 cm intervals from 0 to 10,800 calendar (cal) years B.P. interval (0–513 cm) and at 1 cm intervals from 10,800 to 11,500 cal years B.P. interval (514–540 cm). The planktonic foraminifera *Neogloboquadrina pachyderma* sinistral were analyzed in the lower part of the core (5700–11,500 cal years B.P. interval; 181–540 cm core depth) and *Turborotalita quinqueloba* in the mid part of the core (3500–5700 cal years B.P. interval; 100–171 cm core depth). Owing to the very low abundance of planktonic foraminifera the upper part of the core could not be analyzed. A total of 3–6 specimens of *M. barleeanum* and about 10–20 planktonic specimens of a total weight between 70 and 85 μg were

collected for the Finnigan MAT 251. Some samples were measured on the Finnigan 252, which can measure samples down to 35–50 μg . The measured specimens ranged in size between 100 and 500 μm . Before the measurements, the foraminifera were crushed, cleaned with methanol in an ultrasonic bath and dried at 40°C following the method described by Shackleton and Opdyke [1973], Shackleton et al. [1983] and Duplessy [1978]. The average reproducibility at the GMS laboratory is ± 0.07 for $\delta^{18}\text{O}$ versus Peedee belemnite (PDB) established on replicate measurements of 10 carbonate standards NBS 19 [Coplen, 1996; Ostermann and Curry, 2000].

[13] Eighteen accelerator mass spectrometry (AMS) radiocarbon dates have been measured at the Radiocarbon Laboratory of Uppsala, Sweden (Table 2). The radiocarbon ages were measured on benthic foraminifera except in two levels where bivalve shells were dated. In core NP94-51SC2 the level between 30 and 35 cm was dated twice,

Table 2. Uncorrected AMS ^{14}C Dates and Calibrated Dates Obtained for the NP94-51 Core

Reference Number	Core Depth, cm	AMS ^{14}C Age $\pm 1\sigma$	Calibrated Age Range $\pm 1\sigma$	Cal Age B.P. Used in Age Model	Material Dated
<i>Core NP94-51BC1</i>					
TUa-3407	1–3	515 \pm 55	NC ^a		<i>Nonionellina labradorica</i> , <i>Melonis barleeaanum</i>
TUa-3408	16–18	865 \pm 60	350–470	410	<i>N. labradorica</i> , <i>M. barleeaanum</i>
TUa-3409	30–31	1,085 \pm 65	530–630	580	<i>N. labradorica</i> , <i>M. barleeaanum</i>
<i>Core NP94-51GC1</i>					
TUa-3726	11–15	885 \pm 35	400–485	445	<i>N. labradorica</i> , <i>M. barleeaanum</i> , <i>Buccella frigida</i>
TUa-4079	51–52	1,330 \pm 50	715–845	780	<i>N. labradorica</i> , <i>M. barleeaanum</i> , <i>B. frigida</i>
TUa-4080	90–91	2,015 \pm 40	1,410–1,515	1,465	<i>N. labradorica</i> , <i>M. barleeaanum</i> , <i>B. frigida</i>
TUa-3727	126–127	2,490 \pm 65	1,940–2,110	2,025	<i>N. labradorica</i> , <i>M. barleeaanum</i> , <i>B. frigida</i>
<i>Core NP94-51SC2</i>					
TUa-3739	30–31	3205 \pm 60 ^b			unpaired bivalve shell
TUa-4208	33–35	1,745 \pm 150	1,040–1,350	1,190	<i>N. labradorica</i> , <i>M. barleeaanum</i> , <i>Islandiella norcrossi</i>
TUa-4075	70–71	2,810 \pm 50	2,330–2,485	2,410	<i>N. labradorica</i>
TUa-4076	110–111	4,045 \pm 45	3,850–4,000	3,930	<i>N. labradorica</i>
TUa-4077	191–192	5,720 \pm 50	5,940–6,060	6,015	<i>N. labradorica</i>
TUa-4078	305–306	7,990 \pm 85	8,240–8,440	8,340	mixed benthic foraminifera
TUa-3742	495–496	9,820 \pm 70	10,290–10,620	10,460	unpaired bivalve shell
TUa-3076	525–526	10,255 \pm 95	10,930–11,210	11,015	<i>N. labradorica</i>
TUa-3410	569–570	11,070 \pm 70	12,310–12,660	12,485	<i>N. labradorica</i>
TUa-3075	624–626	13,410 \pm 105	14,430–14,680	14,550	mixed benthic foraminifera
TUa-3587	690–699	14,162 \pm 135	16,030–16,570	16,530	mixed benthic foraminifera

^aNC, not calibrated, not possible to calibrate in the Calib 4.4 program.

^bDate not included in the age model, too old probably because of reworking or transportation.

because of an age reversal (TUa-3739) (Table 2). The second date measured on foraminifera (TUa-4208) indicates no age reversal. We therefore omitted TUa-3739 from the age model of core NP94-51SC2. The AMS ^{14}C ages are calibrated into calendar ages using the calibration program CALIB version 4.4 [Stuiver and Reimer, 1993] with the use of the Marine98 calibration curve [Stuiver et al., 1998a, 1998b] (Table 2). The regional average correction delta R value of 93 ± 23 years for Svalbard (obtained from Marine Reservoir Correction Database in CALIB 4.4) was added to all ages [Stuiver and Braziunas, 1993]. We are aware of the fact that much larger reservoir ages have been published for the deglaciation period from the southern Norwegian Sea [Björck et al., 2003]. However, since there is no published evidence for changes in reservoir ages through the studied period at the northern Svalbard margin we have chosen not to apply any additional correction. The chronology is established using the calibrated calendar ages and assuming uniform sedimentation rate between the dated levels (Figure 3).

[14] The deglaciation and the Holocene periods have been divided based on the most characteristic changes in the benthic foraminifera species distribution [Walton, 1964], and on the combined distribution of IRD, oxygen isotopes, abundance of benthic and planktonic foraminifera. The boundaries are placed at the midpoint of changes. We have accordingly divided the Holocene climatic evolution at the northern Svalbard margin into the major periods: the Younger Dryas–Holocene transition (11,500–10,800 cal years B.P.), the early Holocene (10,800–6800 cal years B.P.), the mid-Holocene transition period (6800–4500 cal years B.P.) and the late Holocene (4500–0 cal years B.P.). This division corresponds well in timing to known divisions of the Holocene climate development from the Nordic Seas

and Icelandic shelf and to the timing of the Holocene Climate Optimum in the same locations [Koç Karpuz and Jansen, 1992; Koç et al., 1993; Andrews and Giraudeau, 2002; Andersen et al., 2004; Knudsen et al., 2004].

4. Results and Interpretation

4.1. Lithological Proxies

[15] Core NP94-51 is mainly composed of fine-grained (silt-clay) sediments showing little variation in grain size and therefore indicating a stable, undisturbed environment at the study site (Figure 4). The only exception to this is the higher percentage of coarser sediments deposited around 17,000 cal years B.P.

[16] The distribution of IRD during the deglaciation has previously been discussed by Koç et al. [2002]. Here we focus on the distribution of IRD during the Holocene (Figure 4). During the early and mid-Holocene, the content of IRD is low and only rarely exceeds 100 grains/g sediment. This indicates that no or very few icebergs melted over the area during this period. An enhanced IRD production is, however, recorded between 10,200 and 10,000 cal years B.P. reflecting increased glacier calving. The IRD concentration shows a weak gradual increase in late Holocene and peaks between 1700 and 1300 cal years B.P. (Figure 4).

4.2. Abundance of Planktonic and Benthic Foraminifera

[17] Several intervals are almost barren of planktonic foraminifera, while benthic foraminifera are present throughout the whole core. The glacial and deglacial interval from 17,000 to 11,000 cal years B.P. is characterized by very low abundances of planktonic and benthic foraminifera

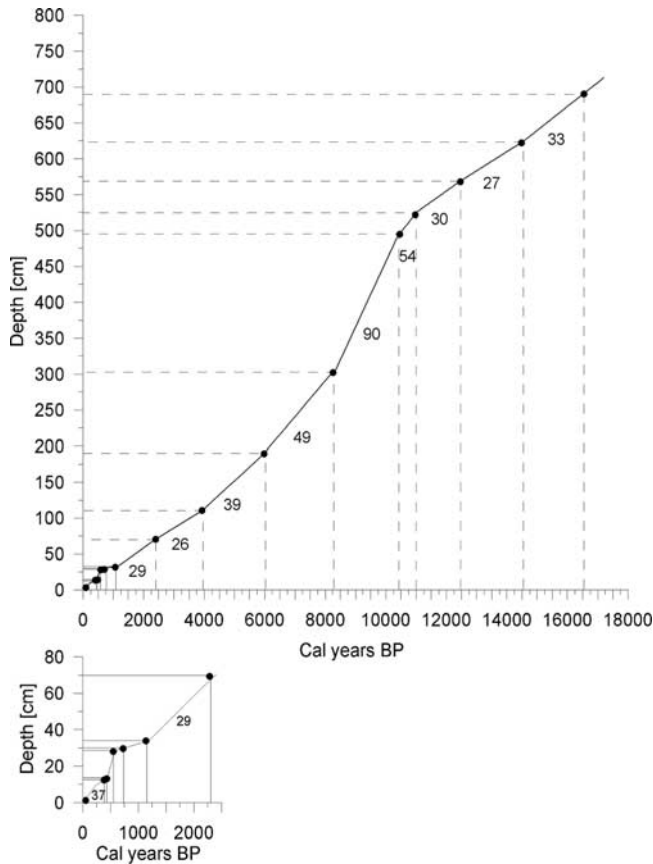


Figure 3. Calibrated calendar ages B.P. plotted versus core depth. Black dots indicate the dated levels. Numbers on the plot show the calculated sedimentation rates in core NP94-51 through the last ~17,200 cal years B.P. The chronology is established using the calibrated calendar ages and assuming uniform sedimentation rate between the dated levels. Details of the last 2500 years are shown in the inset.

(Figure 4) indicating unfavorable ocean conditions and low biological productivity. At 11,000 cal years B.P. a very high peak in number of benthic foraminifera is observed. This peak marks the onset of a generally increasing trend (10,900–9500 cal years B.P.) that coincides with an increased number of planktonic foraminifera (Figure 4), and high accumulation rates (Figure 3). From 9500 to 5400 cal years B.P. the number of benthic foraminifera is relatively high and the distribution pattern is similar to the distribution pattern of planktonic foraminifera (Figure 4). The higher abundance of benthic and planktonic foraminifera suggests improvement in the bottom water conditions and intensified biological productivity. From circa 5400 to 2000 cal years B.P. the concentration of benthic foraminifera remains at the level of ~400 specimens per gram sediment. During the last 2000 years the number of benthic foraminifera declines to ~100 tests/g dry weight sediment and stays low toward the present (Figure 4).

[18] These results indicate that throughout the first half of the Holocene from 10,900 to 5400 cal years B.P. the

bottom water conditions at the site have been generally favorable for the production of benthic foraminifera. Conditions were less favorable during the glacial, the deglaciation and from circa 2000 cal years B.P. to the present.

4.3. Distribution of Benthic Foraminifera Species

[19] The benthic fauna is dominated by species typical of the Arctic continental margin [Polyak and Solheim, 1994; Polyak and Mikhailov, 1996; Hald and Steinsund, 1996; Wollenburg and Mackensen, 1998]. Calcareous species of foraminifera, such as *Cassidulina reniforme*, *Elphidium excavatum* and *Nonionellina labradorica* dominate throughout the core (Figure 5). *Islandiella norcrossi* and *Melonis barleeanum* also reach relatively high percentages of the total fauna (~20–40%).

4.3.1. Glacial and Deglaciation Periods (16,900–11,500 cal years B.P.)

[20] The glacial interval from 17,200 to 14,600 cal years B.P. is characterized by very low concentration and low diversity of the benthic foraminifera (Figures 4 and 5). *Elphidium excavatum* and *C. reniforme* dominate the assemblage (Figure 5). This fauna is typical for glaciomarine environments in proximity to glaciers [Hald et al., 1994; Jennings and Helgadóttir, 1994]. This interval also shows two peaks (maximum 30%) in relative abundance of *Stainforthia loeblichii*, which thrives in cold waters (around 0°C) and within sea ice covered areas [Steinsund, 1994].

[21] From 14,200 to 12,600 cal years B.P. (the Bølling-Allerød interstadial) *Cassidulina neoteretis* dominates the fauna together with a small increase in the abundance of planktonic foraminifera (Figures 4 and 5). *Cassidulina neoteretis* is often associated with higher abundance of planktonic foraminifera [Polyak and Mikhailov, 1996] and is related to phytoplankton blooms [Gooday and Lambshead, 1989]. The strong dominance of *C. neoteretis* during the deglaciation interval is probably related to the inflow of relatively warm Atlantic water masses below a cold and low-saline surface meltwater layer [Mackensen and Hald, 1988; Polyak and Solheim, 1994; Steinsund, 1994; Jennings and Helgadóttir, 1994; Hald and Steinsund, 1996; Rasmussen et al., 1996a, 1996b; Rytter et al., 2002; Jennings et al., 2004]. This distribution is consistent with present occurrences of *C. neoteretis* in surface sediment samples associated with the Atlantic Intermediate Water [Jennings and Helgadóttir, 1994; Lubinski et al., 2001; Rytter et al., 2002; Jennings et al., 2004]. *Cibicides lobatulus* and *M. barleeanum* are also abundant (Figure 5). *Cibicides lobatulus* is associated with stronger current regimes [Korsun and Polyak, 1989; Steinsund, 1994] and *M. barleeanum* is connected to fine-grained sediments rich in organic matter [Korsun and Polyak, 1989; Caralp, 1989; Steinsund, 1994]. At the end of the Bølling-Allerød interstadials *C. neoteretis* decreases and *E. excavatum* increases indicating weakening in the influence of Atlantic water, deterioration of the bottom conditions and stronger glacial influence.

[22] A pronounced increase in the abundance of *N. labradorica* (up to 77% of the total foraminiferal

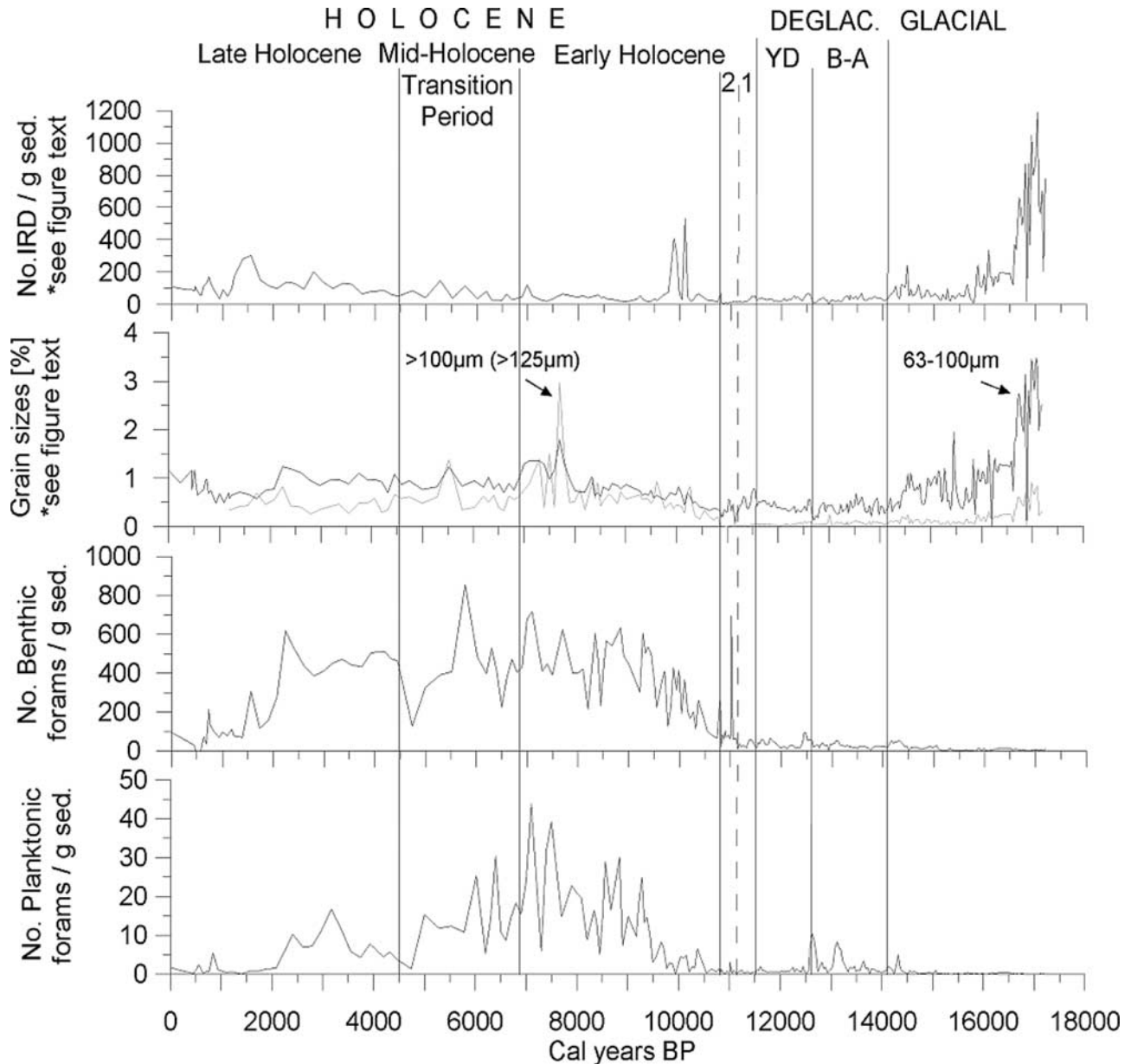


Figure 4. Ice-rafted debris (IRD), grain size distribution, and abundance of benthic and planktonic foraminifera versus calendar age B.P. in NP94-51 core. Note that number of IRD/g sediment was counted in fraction $>125\ \mu\text{m}$ (interval 17,200–10,800 cal years B.P.) and in fraction $>100\ \mu\text{m}$ (interval 10,800 cal years B.P. to 0). In the grain size distribution plots the grey line shows the weight percent of the sieve fraction $>125\ \mu\text{m}$ (interval 17,200–10,800 cal years B.P.) and in fraction $>100\ \mu\text{m}$ (interval 10,800 cal years B.P. to 0), whereas the black line represents the weight percent of the sieve fraction 63–100 μm . Definitions are YD, Younger Dryas; B-A, Bølling-Allerød, and Deglac., deglaciation. Numbers 1 and 2 at the top of Figure 4 indicate the “first” and “second” step at the transition from the YD into the Holocene.

fauna) periodically interrupted by higher occurrences of *C. reniforme*, *E. excavatum* and *S. loeblichii* characterized the Younger Dryas (YD) period at the northern Svalbard margin (Figure 5). *Nonionellina labradorica* correlates positively with the position of the Polar Front and is found on the slopes of banks with high organic content of the sediment [Steinsund, 1994], which suggests that during

most of the YD the Polar Front was in close proximity of the study site [Koç *et al.*, 2002].

4.3.2. Holocene (11,500 cal years B.P. to Present)

4.3.2.1. Younger Dryas–Holocene Transition (11,500–10,800 cal years B.P.)

[23] The transition from Younger Dryas to the Holocene takes place in two steps between 11,500 and 10,800 cal years

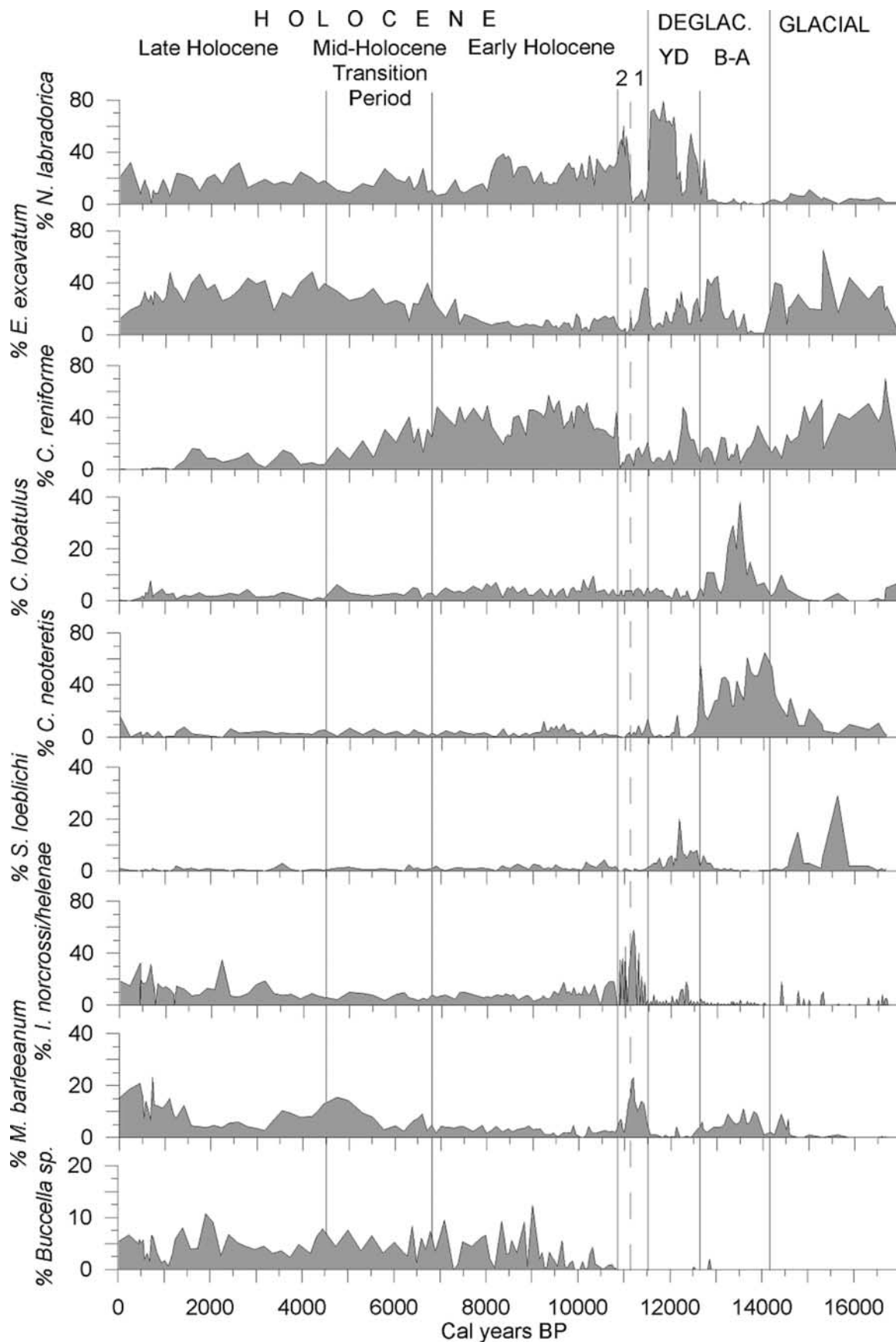


Figure 5. Percent distribution of benthic foraminifera versus calendar age B.P. in core NP94-51.

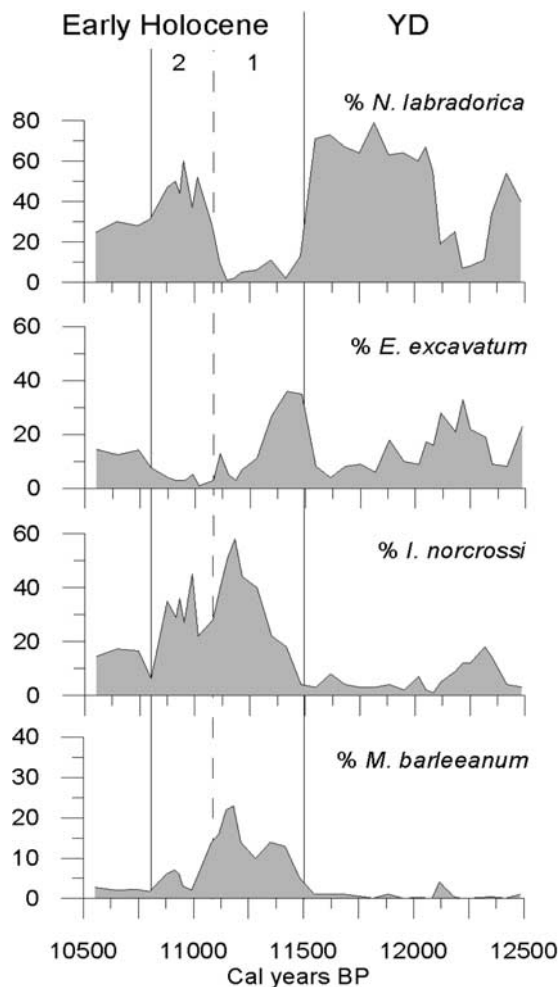


Figure 6. Percent distribution of benthic foraminifera versus calendar age B.P. in the core NP94-51 during the Younger Dryas–early Holocene transition presenting the changes occurring during the “first” and “second” step (marked by numbers 1 and 2 in Figure 6).

B.P. [Koç *et al.*, 2002] (Figures 5 and 6). The Younger Dryas terminates within less than a century at 11,500 cal years B.P. and is marked by a rapid decrease in *N. labradorica* from ~80% to less than 10% of the total fauna (Figure 6). This implies a sudden change in bottom water conditions and probably a northward retreat of the Polar Front from the site. During the first step of the transition between 11,500 and 11,100 cal years B.P. *E. excavatum* peaks followed by *I. norcrossi* and *M. barleeaanum*. *Elphidium excavatum* is found in low and variable temperatures, reduced salinity (30–34‰) and in high-turbidity environments with presence of sea ice [Corliss, 1991; Hald *et al.*, 1994]. This is a very opportunistic species, which often takes advantage of environments unfavorable for most other shelf species [Nagy, 1965; Hald *et al.*, 1994; Jennings *et al.*, 2004]. Relatively high abundance of *E. excavatum* indicates cold and unstable conditions. *Islandiella norcrossi* and *M. barleeaanum* reach their maximum at 11,200 cal years B.P. *Melonis barleeaanum* is considered indicative of increased influx of chilled

Atlantic-derived water to the Arctic Ocean [Korsun and Polyak, 1989; Polyak and Solheim, 1994; Steinsund, 1994] and increased fluxes of organic matter to the sea bottom [Jennings *et al.*, 2004]. In the western Barents Sea, it is recorded at sites with temperatures ranging between 3° and 4°C and salinities above 32‰ [Hald and Steinsund, 1992; Steinsund, 1994]. *Islandiella norcrossi* prefers relatively high and stable bottom salinities [Korsun and Hald, 1998]. Together with *M. barleeaanum* it indicates that conditions changed toward higher salinity and probably slightly higher bottom water temperatures caused by the inflow of Atlantic water. However, the low abundance of *C. neoteretis* indicates that the advection of Atlantic-derived water probably was still reduced over the core site compared to the Bølling-Allerød period (Figure 5). Investigations of modern benthic foraminifera from the northern Icelandic shelf show that *C. neoteretis* dominates in environments where the Atlantic Intermediate Water exist beneath the cold surface layer. In deeper water with the Arctic Water at the surface it is replaced by *M. barleeaanum* [Jennings *et al.*, 2004].

[24] The second step occurs between 11,100 and 10,800 cal years B.P. (Figure 6). The abundance of *I. norcrossi* and *M. barleeaanum* decrease, while *N. labradorica* increases rapidly to ~60% suggesting readvance of the Polar Front toward the study area. However, the conditions are not as severe as during the Younger Dryas. The coexistence of *N. labradorica* and *I. norcrossi*, both preferring high-productivity environments [Steinsund, 1994] indicates well mixed water masses at the front and therefore high organic nutrient content.

4.3.2.2. Early Holocene (10,800–6800 cal years B.P.)

[25] The benthic fauna is characterized by the dominance of *C. reniforme* and *N. labradorica* and the low occurrence of *E. excavatum* (Figure 5). *Cassidulina reniforme* is presently a common species in glaciomarine environments in Svalbard fjords in a distal position from the glacier fronts [Polyak and Solheim, 1994; Hald *et al.*, 1994]. It indicates cold bottom water with lower salinity (>30‰), but not as low as tolerated by *E. excavatum* [Hald and Korsun, 1997]. *Nonionellina labradorica* indicates enhanced organic production [Hald and Vorren, 1987; Korsun *et al.*, 1995]. Together they indicate cold bottom water conditions, but with higher salinity compared to the YD/Holocene transition. The presence of *N. labradorica* further indicates that the Polar Front was in proximity of the core site, whereas the low abundance of *C. neoteretis*, *M. barleeaanum* and *C. lobatulus* indicates a limited advection of Atlantic-derived waters to the site. Compared to the Younger Dryas, the conditions appear more favorable for biological productivity. This is evidenced by the increased abundances of benthic and planktonic foraminifera (Figure 4).

[26] *Buccella* spp. (predominantly *Buccella frigida*) appears at circa 10,850 cal years B.P. and is present throughout the entire Holocene with an average of ~4% (Figure 5). *Buccella* species indicate relatively high seasonal productivity and is related to seasonal sea ice cover [Mudie *et al.*, 1984; Polyak and Solheim, 1994]. Steinsund [1994] found that *Buccella* species prefer temperatures between 0° and 1°C and salinities around 33–34‰.

4.3.2.3. Mid-Holocene Transition Period (6800–4500 cal years B.P.)

[27] The mid-Holocene transition period is characterized by a gradual decrease in the relative abundance of *C. reniforme* and increase in *E. excavatum* (Figure 5). In glaciomarine environments *E. excavatum* commonly replaces *C. reniforme* at the transition from ice-distal to more ice-proximal facies [Hald and Vorren, 1987]. The increase in *E. excavatum* indicates lowered salinity and reduced influence of Atlantic water at the site compared to the early Holocene period.

[28] The percentage of *E. excavatum* reaches nearly 40% of the total foraminiferal fauna toward 4500 cal years B.P. (Figure 5). From circa 5500 to 4000 cal years B.P., *M. barleeanum* rapidly increases in abundance reaching ~15%. *Melonis barleeanum* prefers partly degraded organic matter, commonly originating from redeposition from shallow areas [Caralp, 1989; Corliss, 1991; Korsun and Polyak, 1989]. The higher frequency of *M. barleeanum* is probably a result of a change from more fresh organic matter to more degraded organic matter supply to the bottom waters.

4.3.2.4. Late Holocene (4500 cal years B.P. to Present)

[29] Between 4500 and 1100 cal years B.P., the benthic fauna is dominated by *E. excavatum*, which reaches nearly 50% of the total foraminifera fauna (Figure 5). The observed dominance of *E. excavatum* over *C. reniforme* indicates the presence of cold and low-salinity bottom waters. The abundance of *I. norcrossi*, which prefers relatively high and stable bottom salinities [Polyak and Solheim, 1994; Korsun and Hald, 1998], increases slightly. This species is an epifaunal/shallow infaunal species, which feeds on ice edge algal blooms and therefore is often found close to the sea ice edge [Korsun and Polyak, 1989; Steinsund, 1994]. Therefore the slight increase of this species signals the approach of the sea ice edge.

[30] The faunal changes of the last 1000 years seem to indicate different conditions than the rest of the Holocene. Around 1100 cal years B.P., *C. reniforme* disappears almost completely and *E. excavatum* decreases to ~10%. Concurrent with these changes *M. barleeanum*, *I. norcrossi* and *C. neoteretis* increase in relative abundance (Figure 5). These species indicate increased inflow of chilled Atlantic intermediate water to the area. However, the low concentration of planktonic foraminifera suggests polar conditions at the surface (Figure 4).

4.4. Stable Oxygen Isotopes

[31] The plotted stable oxygen isotope values of the benthic foraminifera *M. barleeanum* and planktonic foraminifera *N. pachyderma* sin. and *T. quinqueloba* have been corrected for their vital effect. An offset of 0.4‰ was used to correct the $\delta^{18}\text{O}$ values of *M. barleeanum* [Duplessy et al., 1980] and a 1‰ offset was used for the planktonic foraminifera *N. pachyderma* sin. and *T. quinqueloba* to correct the $\delta^{18}\text{O}$ values [Duplessy et al., 2001]. The corrected $\delta^{18}\text{O}$ values are adjusted for the ice volume effect [Fairbanks, 1989].

[32] The isotope record of core NP94-51 shows good correspondence with the faunal changes observed in the

same core through the Holocene (Figures 7a–7d). Between 11,500 and 10,800 cal years B.P. both the benthic and the planktonic isotope values are low indicating the presence of low-salinity waters at the northern Svalbard margin. In this period the surface waters are covered with sea ice and influenced by meltwater from surrounding glaciers, whereas the bottom waters are characterized by high turbidity and low salinity and temperature as indicated by the abundance of *E. excavatum*. From 10,800 to 1000 cal years B.P. the benthic isotope record shows an overall 0.8‰ increase in the $\delta^{18}\text{O}$ values (Figure 7a).

[33] Higher $\delta^{18}\text{O}$ values and an increase in the dominance of *E. excavatum* (Figure 7d), together with a simultaneous decrease in the abundance of *C. reniforme* (Figure 7c), reflect cooling of bottom waters. The planktonic $\delta^{18}\text{O}$ record is highly fluctuating in the period between 10,800 and 3500 cal years B.P. pointing to unstable subsurface waters conditions (Figure 7b). The past 1000 years show high benthic $\delta^{18}\text{O}$ values with some fluctuations indicating variable conditions (Figure 7a).

5. Paleooceanography and Climate Development During the Last ~17,200 cal Years B.P. at the Northern Svalbard Continental Margin

[34] Fully glaciomarine conditions were established in the Hinlopen Trough 13.9–13.7 ^{14}C kyr B.P. (16,900–16,500 cal years B.P.) (Figure 5). The Late Weichselian ice sheet in the Svalbard region extended onto the shelf [Svendsen and Mangerud, 1992; Lambeck, 1996; Landvik et al., 1998; Svendsen et al., 1999; Mangerud et al., 2002; Forman et al., 2004]. The strong IRD signal in core NP94-51 indicates that the disintegration of the ice, grounded in the Hinlopen Trough during the Last Glacial Maximum (LGM) was initiated before 13.9–13.7 ^{14}C kyr B.P. Hence the disintegration of the Svalbard ice sheet and possibly the Barents Sea ice sheet started before this time, which is in agreement with other studies from the Eurasian Arctic continental margin [e.g., Cadman, 1996; Knies et al., 2000; Vogt et al., 2001].

[35] The inflow of the warm Atlantic water along the eastern margin of the Nordic seas after the LGM was reinitiated at 13.4 ^{14}C kyr B.P. (circa 16,000 cal years B.P.) [Koç Karpuz and Jansen, 1992; Koç et al., 1993]. Farther north along the western slope of the Barents Sea the surface warming was delayed by circa 1000 years and is dated to 12.6 ^{14}C kyr B.P. (circa 15,000 cal years B.P.) [Hald et al., 1996; Koç et al., 1996]. At the northern shelf of Svalbard (80°N), the initial strong advection of Atlantic water was recorded in the bottom waters simultaneously with the surface warming at the Barents Slope [Koç et al., 2002]. The implication is that once the warm surface flow reached 72°N it continued farther north and into the Arctic as a relatively strong subsurface intermediate flow as indicated by high relative abundance of *C. neoteretis* (Figure 5).

[36] All along the pathway of the North Atlantic Current up to the Barents Slope the Bølling-Allerød interstadial is regarded as warm. However, it was not as warm as the Holocene Climate Optimum from the Nordic Seas [Koç et

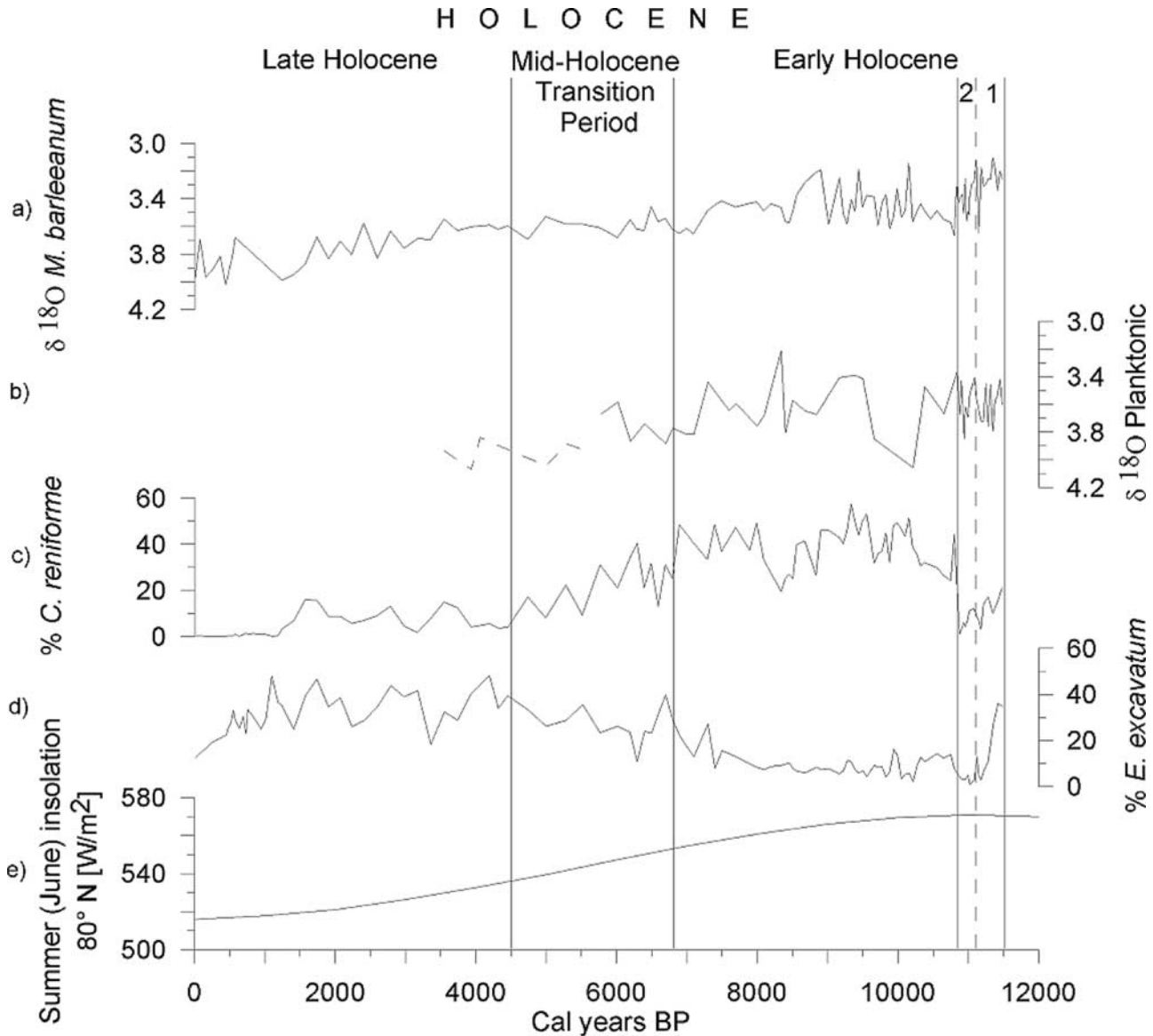


Figure 7. Holocene stable oxygen isotope records: (a) $\delta^{18}\text{O}$ of benthic foraminifera *M. barleeaanum* and (b) $\delta^{18}\text{O}$ of planktonic foraminifera. Dashed line represents measurements done on *T. quinqueloba*, and the solid line represents measurements done on *N. pachyderma* (sin). Plotted variations in percentage abundance of benthic foraminifera (c) *C. reniforme* and (d) *E. excavatum*, and (e) summer insolation curve for June for 80°N in W/m^2 [Berger, 1978].

al., 1996]. In comparison to this, the Bølling-Allerød interstadial stands out as the interval with the strongest advection of Atlantic water in the bottom waters of the northern shelf of Svalbard as indicated by the highest abundance of *C. neoteretis* recorded in the studied interval (Figure 5). The biological productivity is very low at this time because of the existing sea ice cover as indicated by the total absence of diatom species [Koç et al., 2002]. We therefore conclude that the strongest subsurface influx of Atlantic-derived water over the core site took place below a sea ice covered surface during the Bølling-Allerød interstadial.

[37] The Younger Dryas period is recorded as an abrupt and pronounced cooling all along the pathway of the NAC in the Norwegian Sea [Koç et al., 1993; Klitgaard-Kristensen et al., 2001; Ebbesen and Hald, 2004] including the branch at the northern shelf of Svalbard. The YD cooling north of Svalbard is characterized by the presence of sea ice, influence of meltwater, cold water masses at the surface and bottom, and the vicinity of the Polar Front. The first occurrence of diatom species related to sea ice at the marginal ice zone and to the Arctic water is also recorded during YD at the northern Svalbard margin at 10.8 ^{14}C kyr B.P. (circa 12,700 cal years B.P.).

Diatoms are not present in surface waters before the YD indicating extensive sea ice cover in the area during the Bølling-Allerød interstadial [Koç *et al.*, 2002].

[38] The two-step warming into the Holocene recorded in several other records from the Nordic Seas [e.g., Koç Karpuz and Jansen, 1992; Hald and Aspeli, 1997] is also clearly discernible in core NP94-51. It correlates in time with the YD-Preboreal oscillation [e.g., Björck *et al.*, 1996, 1997]. The transition is accompanied by an increase of *M. barleeanum* and *I. norcrossi/helenae* and an increase in the number of benthic foraminifera (Figures 4, 5 and 6). However, the lack of significant increase in *C. neoteretis* implies that the influence of Atlantic-derived bottom water was modest at the transition to the Holocene at the northern Svalbard margin. The increase in Atlantic water inflow was short-lived, and in the period from circa 11,100 to 10,800 cal years B.P. the Polar Front reapproached the area leading to conditions comparable to those of the Younger Dryas cold period with the ice edge close by (Figures 5 and 6). The stable oxygen isotope data show low values at this interval (Figures 7a and 7b). The presence of enhanced meltwater may have contributed to the recorded instability at the transition.

[39] After 10,800 cal years B.P. the surface and bottom waters conditions remained in a glacial distal environment with seasonal sea ice cover, proximity of the Polar Front and low ice rafting. This implies in general that the inflow of Atlantic-derived water at the northern Svalbard margin through the Holocene did not result in strong temperature changes. As such, the conditions at the northern Svalbard margin deviate slightly from the surface conditions in the Nordic Seas where the early Holocene is a period of climatic optimum conditions with up to 4–5°C warmer SSTs than at present [Koç *et al.*, 1993; Andersen *et al.*, 2004]. Evidences for the Holocene Climate Optimum conditions are registered as far north as the western slope of the Barents Sea shelf [Hald *et al.*, 1996; Koç *et al.*, 1996; Sarnthein *et al.*, 2003]. The only indication of a climate optimum in Hinlopen is the strong seasonal productivity of benthic and planktonic foraminifera existing until 2000 cal years B.P. In addition, the overall shift from *C. reniforme* preferring higher salinity to *E. excavatum* tolerating lower salinities suggest change in bottom water conditions related to influence of Atlantic water. The lack of evidence in the form of warm water foraminifera species in the Hinlopen Trough may indicate either that the inflow of the Atlantic water was not strong enough during this period or that the observed surface warming in the Nordic Seas was mainly due to high summer insolation. Further, if mixing of warm water with colder Arctic water took place between the Barents slope and the northern Svalbard margin this would lead to inflow of cooler waters. Occurrences of thermophilous molluscs (e.g., *Mytilus edulis*) however, indicate a climatic optimum in coastal waters west and north of Svalbard at circa 8700–7700 cal years B.P. and that ameliorated conditions lasted to about 3500 cal years B.P. [Salvigsen *et al.*, 1992; Salvigsen, 2002]. This could also be interpreted as a response to the high summer insolation and associated warming of shallow coastal waters.

[40] The trend of increasing $\delta^{18}\text{O}$ values throughout the Holocene reflects primarily declining temperatures. This corresponds well with the change from higher abundances of *C. reniforme* in the early Holocene to a dominance of *E. excavatum* during the late Holocene. This distribution pattern of benthic foraminiferal species and the timing of changes in the assemblages during the Holocene are very similar to other sites that are under the influence of the Atlantic-derived waters at the Eurasian margin and fjords: the Franz Victoria Trough [Duplessy *et al.*, 2001; Lubinski *et al.*, 2001], the St. Anna Trough [Hald *et al.*, 1999; Lubinski *et al.*, 2001] at the northern margin of the Barents Sea, and in the Van Mijenfjord, western Svalbard [Hald *et al.*, 2004]. The similarity in this region with the oceanographic development observed at the surface waters farther south in the eastern Norwegian Sea [Birks and Koç, 2002; Andersen *et al.*, 2004] indicates a close coupling of these two regions via the Norwegian Atlantic Current. However, the overall distribution pattern of *C. reniforme* is also similar to the long-term trend in the summer June insolation curve [Berger, 1978]. The general similarity between the two curves (Figures 7c and 7d) leads us to speculate, whether the decreasing abundance of *C. reniforme* and increasing abundance of *E. excavatum* reflecting progressively harsher conditions through the Holocene, could be related to the decreasing influx of solar radiation (Figures 7c–7e).

[41] The content of IRD is generally low through the Holocene. Dowdeswell [1989] suggested that during the Holocene icebergs were restricted to and melted in the inner fjord environments in the eastern Polar North Atlantic and Svalbard. A pronounced peak in the concentration of IRD is recorded between 10,200 and 10,000 cal years B.P. (Figure 4). A similar peak in IRD was recorded by Duplessy *et al.* [2001] in the northern Barents Sea (Franz Victoria Trough) at circa 10,000 cal years B.P. In the western Svalbard and western Barents Sea the ice retreated rapidly around 10 ^{14}C kyr B.P. (~11,100–11,500 cal years B.P.) [Svendsen and Mangerud, 1992; Landvik *et al.*, 1998]. The increased ice rafting at the northern Barents Sea margin during the early Holocene may reflect the final collapse of the northern Svalbard-Barents Sea Ice Sheet. The weak but gradual increase in IRD during the late Holocene (Figure 4) correlates well with the general deterioration of climate indicated by the changes in the foraminifera faunas and the increase in $\delta^{18}\text{O}$ values (Figures 5 and 7). The intensified iceberg production was related to the advances of the glaciers on Svalbard and enhanced calving [Elverhøi *et al.*, 1995; Svendsen and Mangerud, 1997]. The Holocene ice rafting pattern follows the glacier development on Svalbard inferred from investigations of terrestrial sediments. These findings suggest significantly reduced glacier cover during the early and mid Holocene [Svendsen and Mangerud, 1992] followed by advance of the glaciers during the late Holocene [Svendsen and Mangerud, 1997].

[42] Compared to the earlier part of the Holocene, the last circa 1100 years seems to be more environmentally unstable and probably warmer at the bottom waters at the northern Svalbard margin (Figure 5). Ice rafting decreased, the productivity of foraminifera was low and the sedimentation rate increased (Figures 3 and 4), suggesting Atlantic water

influence at the bottom and probably seasonal sea ice cover. These conditions seem to be similar to the Bølling-Allerød conditions. However, one difference between the two periods is that the abundance of *C. neoteretis* was low during the last 1100 years, and only shows increased abundance in the surface sample (Figure 5). The species (as *C. teretis*) has also been found living northeast of Svalbard in surface samples from 300 to 1400 m water depth (sieve fraction >125 μm) [Wollenburg and Mackensen, 1998]. The short reappearance of *M. edulis* in Svalbard waters at circa 1000 cal years B.P., during the so-called Little Climate Optimum [Salvigsen et al., 1992; Salvigsen, 2002], also indicates return of warmer conditions. The new finding of *M. edulis* in August 2004 in Isfjorden, western Svalbard [Berge et al., 2005] probably confirms the present warming signal in the Arctic marine environment. Evidently, the influence of Atlantic water increases, but conditions have also become more unstable compared to the period between circa 10,800 and 1100 cal years B.P. Increased warmth at the northern Svalbard margin is in good accordance with the recorded relatively high temperature (3.5°–4°C) of the Atlantic Layer situated only 25 m below the surface in summer 1994 (Figure 2), and the observed tendencies for warming in the Arctic [e.g., Schauer et al., 2004; Johannessen et al., 2004; Comiso and Parkinson, 2004].

6. Conclusions

[43] We have presented our Holocene record together with the glacial and deglaciation record from the same site. We aimed to elucidate the variations in the inflow of Atlantic water into the Arctic Ocean within the Holocene period in comparison to the deglaciation.

[44] Our main conclusions on the history of Atlantic inflow into the Arctic Ocean are the following.

[45] 1. The strongest subsurface inflow of relatively warm Atlantic water below a cold and low-saline surface meltwater layer occurred at 12.6 ^{14}C kyr B.P. (circa 15,000 cal years B.P.), and it remained strong during the Bølling-Allerød interstadial. This period is, however, characterized by a very low productivity and extensive sea ice cover over the site.

[46] 2. During most of the Younger Dryas the Polar Front was situated in the vicinity of the core site. The record of ice rafted debris is similar to the IRD record from the Bølling-

Allerød interstadial, but cold water masses prevailed. The subsurface inflow of Atlantic water was reduced compared to the Bølling-Allerød interstadial. The end of the YD was marked by the northward retreat in the position of the Polar Front.

[47] 3. During the two-step transition from the YD to the Holocene a short-lived (~300 years) stronger influence of chilled Atlantic-derived water was detected, before conditions returned to YD-like conditions after 10,800 cal years B.P.

[48] 4. During the early Holocene the influence of the more saline, but still cold Atlantic-derived water increased. The surface conditions were polar, but ameliorated and favorable enough for relatively high seasonal productivity. The Polar Front was positioned in close vicinity of the site. The site was in a glacial distal environment with seasonal sea ice cover and no significant iceberg production or with very few icebergs melting over the core site. The Holocene Climate Optimum is less evident as a temperature signal at the northern Svalbard margin than in the east Norwegian Sea.

[49] 5. The mid-Holocene transition period is marked by a gradual decrease in the inflow of Atlantic-derived water.

[50] 6. During the late Holocene the inflow of warm water masses carried by the West Spitsbergen Current decreased to a very low level. Conditions at the surface and bottom waters were polar with low salinity and extensive sea ice cover and marked by the readvance of glaciers on Svalbard.

[51] 7. During the last ~1100 years climatic conditions improved and the inflow of Atlantic-derived water increased, while surface water was generally of polar conditions.

[52] **Acknowledgments.** The University Centre in Svalbard, the Norwegian Polar Institute, and the Norwegian Research Council funded this study. This study is a part of NRC-funded MACESIZ project. The manuscript benefited from the constructive comments of Lisa Sloan, John T. Andrews, and one anonymous reviewer. Anders Solheim and Carl Fredric Forsberg are acknowledged for leading the cruise to the northern Svalbard margin in 1994. Radiocarbon dating was performed at the Radiocarbon Laboratories in Trondheim and Uppsala. Ulysses Ninnemann and Rune Sørås, from the GSM Laboratory at the University of Bergen and the Bjerknes Centre for Climate Research, are gratefully acknowledged for helping with the stable isotope measurements. We thank Ragnheid Skogseth and Malin Daase for help with some of the figures and Gaute Mikalsen for discussion on the stable isotope records.

References

- Aagaard, K., and E. C. Carmack (1989), The role of sea ice and other freshwater in the Arctic circulation, *J. Geophys. Res.*, *94*, 14,485–14,498.
- Aagaard, K., and P. Greisman (1975), Towards new mass and heat budgets in the Arctic Ocean, *J. Geophys. Res.*, *80*, 3821–3827.
- Aagaard, K., A. Foldvik, and S. R. Hillman (1987), The West Spitsbergen Current: Disposition and water mass transformation, *J. Geophys. Res.*, *92*, 3778–3784.
- Andersen, C., N. Koç, A. Jennings, and J. T. Andrews (2004), Nonuniform response of the major surface currents in the Nordic Seas to insolation forcing: Implications for the Holocene climate variability, *Paleoceanography*, *19*, PA2003, doi:10.1029/2002PA000873.
- Andrews, J. T., and J. Giraudeau (2002), Multi-proxy records showing significant Holocene environmental variability: The inner N. Iceland shelf (Húnaflói), *Quat. Sci. Rev.*, *22*, 175–193.
- Armstrong, R. L., and M. J. Brodzik (2001), Recent Northern Hemisphere snow extent: A comparison of data derived from visible and microwave satellite sensors, *Geophys. Res. Lett.*, *28*(19), 3673–3676.
- Berge, J., G. Johnsen, F. Nilsen, B. Gulliksen, and D. Slagstad (2005), Ocean temperature oscillations enable reappearance of blue mussels *Mytilus edulis* in Svalbard after a 1000 yr absence, *Mar. Ecol. Prog. Ser.*, in press.
- Berger, A. (1978), Long-term variations of caloric insolation resulting from the Earth's orbital elements, *Quat. Res.*, *9*, 139–167.
- Birks, C. J. A., and N. Koç (2002), A high-resolution diatom record of late-Quaternary sea-surface temperatures and oceanographic conditions from the eastern Norwegian Sea, *Boreas*, *31*, 323–344.
- Björck, S., et al. (1996), Synchronized terrestrial-atmospheric deglacial records around the North Atlantic, *Science*, *274*, 1155–1160.

- Björck, S., M. Rundgren, O. Ingólfsson, and S. Funder (1997), The Preboreal oscillation around the Nordic Seas: Terrestrial and lacustrine responses, *J. Quat. Sci.*, 12(6), 455–465.
- Björck, S., N. Koç, and G. Skog (2003), Consistently large marine reservoir ages in the Norwegian Sea during the last deglaciation, *Quat. Sci. Rev.*, 22, 429–435.
- Cadman, V. (1996), Glaciomarine sedimentation and environments during the late Weichselian and Holocene in the Bellsund Trough and Van Keulenfjorden, Svalbard, Ph.D. thesis, 250 pp., Univ. of Cambridge, U.K.
- Caralp, M. H. (1989), Abundance of *Bulimia exilis* and *Melonis barleeianum*: Relationship to the quality of marine organic matter, *Geo. Mar. Lett.*, 9, 37–43.
- Chapman, W. L., and J. E. Walsh (1993), Recent variations of sea ice and air temperature in high latitudes, *Bull. Am. Meteorol. Soc.*, 74, 33–47.
- Comiso, J. C. (2002), A rapidly declining perennial sea ice cover in the Arctic, *Geophys. Res. Lett.*, 29(20), 1956, doi:10.1029/2002GL015650.
- Comiso, J. C. (2003), Warming trends in the Arctic from clear sky satellite observations, *J. Clim.*, 16, 3498–3510.
- Comiso, J. C., and C. L. Parkinson (2004), Satellite-observed changes in the Arctic, *Phys. Today*, 57(8), 38–44.
- Coplen, T. (1996), New guidelines for reporting stable hydrogen, carbon, and oxygen-ratio data, *Geochim. Cosmochim. Acta*, 60(17), 3359–3360.
- Corliss, B. H. (1991), Morphology and microhabitat preferences of benthic foraminifera from the north-west Atlantic Ocean, *Mar. Micropaleontol.*, 17, 195–236.
- Dickson, R., T. J. Osborn, J. W. Hurrell, J. Meincke, J. Blindheim, B. Adlandsvik, T. Vinje, G. Alekseev, and W. Maslowski (2000), The Arctic Ocean response to the North Atlantic Oscillation, *J. Clim.*, 13, 2671–2696.
- Dowdeswell, J. A. (1989), On the nature of Svalbard icebergs, *J. Glaciol.*, 35, 224–234.
- Duplessy, J. C. (1978), Isotope studies, in *Climate Change*, edited by J. Gribbin, pp. 46–67, Cambridge Univ. Press, New York.
- Duplessy, J. C., J. Moyes, and C. Pujol (1980), Deep water formation in the North Atlantic Ocean during the last ice age, *Nature*, 286, 479–482.
- Duplessy, J. C., E. Ivanova, I. Murdmaa, M. Paterné, and L. Labeyrie (2001), Holocene paleoceanography of the northern Barents Sea and variations of the northward heat transport by the Atlantic Ocean, *Boreas*, 30, 2–16.
- Ebbesen, H., and M. Hald (2004), Unstable Younger Dryas climate in the northeast North Atlantic, *Geology*, 32, 673–676.
- Elverhøi, A., J. I. Svendsen, A. Solheim, E. S. Andersen, J. Milliman, J. Mangerud, and R. L. Hooke (1995), Late Quaternary sediment yield from the high Arctic Svalbard area, *J. Geol.*, 103, 1–17.
- Fairbanks, R. G. (1989), A 17000-years glacio-eustatic sea level record: Influence of glacial melting rates on the Younger Dryas event and deep-ocean circulation, *Nature*, 342, 637–742.
- Forman, S. L., D. J. Lubinski, Ó. Ingólfsson, J. J. Zeeberg, J. A. Snyder, M. J. Siebert, and G. G. Matishov (2004), A review of postglacial emergence on Svalbard, Franz Josef Land and Novaya Zemlya, northern Eurasia, *Quat. Sci. Rev.*, 23, 1391–1434.
- Gooday, A. J., and P. J. D. Lamshead (1989), Influence of seasonally deposited phytodetritus on benthic foraminifera populations in the bathyal northeast Atlantic: The species response, *Mar. Ecol. Prog. Ser.*, 58, 53–67.
- Grotedefend, K., K. Logemann, D. Quadfasel, and S. Ronski (1998), Is the Arctic Ocean warming?, *J. Geophys. Res.*, 103, 27,679–27,687.
- Hald, M., and R. Aspelí (1997), Rapid climatic shifts on the northern Norwegian Sea during the last deglaciation and the Holocene, *Boreas*, 26, 15–28.
- Hald, M., and S. Korsun (1997), Distribution of modern benthic foraminifera from fjords of Svalbard, European Arctic, *J. Foraminiferal Res.*, 27, 101–122.
- Hald, M., and P. I. Steinsund (1992), Distribution of surface sediment benthic foraminifera in the southwestern Barents Sea, *J. Foraminiferal Res.*, 22, 347–362.
- Hald, M., and P. I. Steinsund (1996), Benthic foraminifera and carbonate dissolution in the surface sediments of the Barents and Kara Seas, *Ber. Polarforsch.*, 212, 285–307.
- Hald, M., and T. O. Vorren (1987), Foraminiferal stratigraphy and environment of late Weichselian deposits on the continental shelf off Troms, northern Norway, *Mar. Micropaleontol.*, 12, 129–160.
- Hald, M., P. I. Steinsund, T. Dokken, S. Korsun, L. Polyak, and R. Aspelí (1994), Recent and late Quaternary distribution of *Elphidium excavatum* f. *clavatum* in the Arctic seas, *Cushman Found. Spec. Publ.*, 32, 141–153.
- Hald, M., T. Dokken, and S. Hagen (1996), Paleoceanography of the European Arctic margin during the last deglaciation, in *Late Quaternary Paleoceanography of the North Atlantic Margins*, edited by J. T. Andrews et al., *Geol. Soc. Spec. Publ.*, 111, 275–287.
- Hald, M., V. Kolstad, L. Polyak, S. L. Forman, F. A. Herlihy, G. Ivanov, and A. Nescheretov (1999), Late-glacial and Holocene paleoceanography and sedimentary environments in the St. Anna Trough, Eurasian Arctic Ocean margin, *Palaeogeogr. Palaeoclimatol. Palaeoecol.*, 146, 229–249.
- Hald, M., T. Dahlgren, T.-E. Olsen, and E. Lebesbye (2001), Late Holocene paleoceanography in Van Mijenfjorden, Svalbard, *Polar Res.*, 20, 23–35.
- Hald, M., H. Ebbesen, M. Forwick, F. Godtliebsen, L. Khomeiko, S. Korsun, L. Ringstad Olsen, and T. O. Vorren (2004), Holocene paleoceanography and glacial history of the West Spitsbergen area, Euro-Arctic margin, *Quat. Sci. Rev.*, 23, 2075–2088.
- Hisdal, V. (1998), *Svalbard Nature and History*, *Polarhåndbok*, vol. 12, 123 pp., Nor. Polarinst., Oslo.
- Jennings, A. E., and G. Helgadóttir (1994), Foraminiferal assemblages from the fjords and shelf of eastern Greenland, *J. Foraminiferal Res.*, 24, 123–144.
- Jennings, A. E., N. J. Weiner, G. Helgadóttir, and J. T. Andrews (2004), Modern foraminiferal faunas of the southwestern to northern Iceland shelf: Oceanographic and environmental controls, *J. Foraminiferal Res.*, 34, 180–207.
- Johannessen, O. M., E. V. Shalina, and M. W. Miles (1999), Satellite evidence for an Arctic sea ice cover in transformation, *Science*, 286, 1937–1939.
- Johannessen, O. M., et al. (2004), Arctic climate change: Observed and modelled temperature and sea-ice variability, *Tellus, Ser. A*, 56, 328–341.
- Klitgaard-Kristensen, D., H. P. Sejrup, and H. Hafliðason (2001), The last 18 kyr fluctuations in Norwegian Sea surface conditions and implications for the magnitude of climatic change: Evidence from the North Sea, *Paleoceanography*, 16, 455–467.
- Knies, J., N. Nowaczyk, C. Müller, C. Vogt, and R. Stein (2000), A multiproxy approach to reconstruct the environmental changes along the Eurasian continental margin over the last 150,000 years, *Mar. Geol.*, 163, 317–344.
- Knudsen, K. L., and W. E. N. Austin (1996), Late glacial foraminifera, in *Late Quaternary Paleoceanography of the North Atlantic Margins*, edited by J. T. Andrews et al., *Geol. Soc. Spec. Publ.*, 111, 7–10.
- Knudsen, K. L., H. Jiang, E. Jansen, J. Eiríksson, J. Heinemeier, and M.-S. Seidenkrantz (2004), Environmental changes off north Iceland during the deglaciation and the Holocene: Foraminifera, diatoms and stable isotopes, *Mar. Micropaleontol.*, 50, 273–305.
- Koç, N., E. Jansen, and H. Hafliðason (1993), Paleoceanographic reconstructions of surface ocean conditions in the Greenland, Iceland and Norwegian Seas through the last 14 ka based on diatoms, *Quat. Sci. Rev.*, 12, 115–140.
- Koç, N., E. Jansen, M. Hald, and L. Labeyrie (1996), Late-glacial–Holocene sea surface temperatures and gradients between the North Atlantic and the Norwegian Sea: Implications for the Nordic heat pump, in *Late Quaternary Paleoceanography of the North Atlantic Margins*, edited by J. T. Andrews et al., *Geol. Soc. Spec. Publ.*, 111, 177–185.
- Koç, N., D. Klitgaard-Kristensen, K. Hasle, C. F. Forsberg, and A. Solheim (2002), Late glacial paleoceanography of Hinlopen Strait, northern Svalbard, *Polar Res.*, 21, 307–314.
- Koç Karpuz, N., and E. Jansen (1992), A high-resolution diatom record of the last deglaciation from the SE Norwegian Sea: A documentation of rapid climatic changes, *Paleoceanography*, 7, 499–520.
- Korsun, S. A., and M. Hald (1998), Modern benthic foraminifera off Novaya Zemlya tide-water glaciers, Russian Arctic, *Arct. Alp. Res.*, 30(1), 61–77.
- Korsun, S. A., and L. V. Polyak (1989), Distribution of benthic foraminiferal morphogroups in the Barents Sea, *Oceanology, Engl. Transl.*, 29, 838–844.
- Korsun, S. A., I. Pogodina, S. L. Forman, and D. Lubinski (1995), Recent foraminifera in glaciomarine sediments from three Arctic fjords of Novaya Zemlya and Svalbard, *Polar Res.*, 14, 15–31.
- Kowalik, Z., and A. Y. Proshutinsky (1995), Topographic enhancement of tidal motion in the western Barents Sea, *J. Geophys. Res.*, 100, 2613–2637.
- Lambeck, K. (1996), Limits on the areal extent of the Barents Sea ice sheet in late Weichselian time, *Global Planet. Change*, 12, 41–51.
- Landvik, J. Y., S. Bondevik, A. Elverhøi, W. Fjeldskaar, J. Mangerud, O. Salvigsen, M. J. Siebert, J. I. Svendsen, and T. O. Vorren (1998), The Last Glacial Maximum of Svalbard and the Barents Sea area: Ice sheet extent and configuration, *Quat. Sci. Rev.*, 17, 43–75.
- Lubinski, D. J., S. Korsun, L. Polyak, S. L. Forman, S. J. Lehman, F. A. Herlihy, and G. H. Miller (1996), The last deglaciation of the Franz Victoria Trough, northern Barents Sea, *Boreas*, 25, 89–100.
- Lubinski, D. J., L. Polyak, and S. L. Forman (2001), Freshwater and Atlantic water inflows to the deep northern Barents and Kara seas

- since ca 13 ¹⁴C ka: Foraminifera and stable isotopes, *Quat. Sci. Rev.*, 20, 1851–1879.
- Mackensen, A., and M. Hald (1988), *Cassidulina teretis* Tappan and *C. laevigata* d'Orbigny: Their modern and late Quaternary distribution in northern seas, *J. Foraminiferal Res.*, 18, 16–24.
- Mangerud, J., V. Astakhov, and J.-I. Svendsen (2002), The extent of the Barents-Kara ice sheet during the Last Glacial Maximum, *Quat. Sci. Rev.*, 21, 111–119.
- Manley, T. O. (1995), Branching of Atlantic Water within the Greenland-Spitsbergen passage: An estimate of recirculation, *J. Geophys. Res.*, 100, 20,627–20,634.
- Mudie, P. J., C. E. Keen, I. A. Hardy, and G. Vilks (1984), Multivariate-analysis and quantitative paleoecology of benthic foraminifera in surface and late Quaternary shelf sediments, northern Canada, *Mar. Micropaleontol.*, 8, 283–313.
- Nagy, J. (1965), Foraminifera in some bottom samples from shallow waters in Vestspitsbergen, *Aarb. Nor. Polarinst.*, 1963, 109–127.
- Ostermann, D. R., and W. B. Curry (2000), Calibration of stable isotopic data: An enriched $\delta^{18}\text{O}$ standard used for source gas mixing detection and correction, *Paleoceanography*, 15, 353–360.
- Pfirman, S. L., D. Bauch, and T. Gammelsrød (1994), The Northern Barents Sea: Water mass distribution and modification, in *The Polar Oceans and Their Role in Shaping the Global Environment*, *Geophys. Monogr. Ser.*, vol. 85, edited by O. M. Johannessen, R. D. Muench, and J. E. Overland, pp. 77–94, AGU, Washington, D. C.
- Polyak, L., and V. Mikhailov (1996), Post-glacial environments of the southeastern Barents Sea: Foraminiferal evidence, in *Late Quaternary Paleoenvironment of the North Atlantic Margins*, edited by J. T. Andrews et al., *Geol. Soc. Spec. Publ.*, 111, 323–337.
- Polyak, L., and A. Solheim (1994), Late- and postglacial environments in the northern Barents Sea, west of Franz Josef Land, *Polar Res.*, 13, 197–207.
- Quadfasel, D., A. Sy, and B. Rudels (1993), A ship of opportunity section to the North Pole: Upper ocean temperature observations, *Deep Sea Res., Part I*, 40, 777–789.
- Rasmussen, T. L., E. Thomsen, L. Labeyrie, and T. C. E. van Weering (1996a), Circulation changes in the Faeroe-Shetland Channel correlating with cold events during the last glacial period (58–10 ka), *Geology*, 24, 937–940.
- Rasmussen, T. L., E. Thomsen, T. C. E. van Weering, and L. Labeyrie (1996b), Rapid changes in surface and deep water conditions at the Faeroe Margin during the last 58,000 years, *Paleoceanography*, 11, 757–771.
- Rudels, B. (1987), On the mass balance of the Polar Ocean, with the emphasis on the Fram Strait, *Skr. Nor. Polarinst.*, 188, 53 pp.
- Rudels, B., H. J. Friedrich, and D. Quadfasel (1999), The Arctic Circumpolar boundary current, *Deep Sea Res., Part II*, 46, 1023–1062.
- Rytter, F., K. L. Knudsen, M.-S. Seidenkrantz, and J. Eiriksson (2002), Modern distribution of benthic foraminifera on the northern Icelandic shelf and slope, *J. Foraminiferal Res.*, 32, 217–244.
- Saloranta, T. M., and P. M. Haugan (2001), Inter-annual variability in the hydrography of Atlantic water northwest of Svalbard, *J. Geophys. Res.*, 106, 13,931–13,943.
- Salvigsen, O. (2002), Radiocarbon-dates *Mytilus edulis* and *Modiolus modiolus* from northern Svalbard: Climatic implications, *Nor. Geogr. Tidsskr.*, 56, 56–61.
- Salvigsen, O., S. L. Forman, and G. H. Miller (1992), Thermophilous molluscs on Svalbard during the Holocene and their palaeoclimatic implications, *Polar Res.*, 11, 1–10.
- Sarnthein, M., S. van Kreveld, H. Erlenkeuser, P. M. Grootes, M. Kucera, U. Pflaumann, and M. Schulz (2003), Centennial-to-millennial-scale periodicities of Holocene climate and sediment injections off the western Barents shelf, 75°N, *Boreas*, 32, 447–461.
- Schauer, U., E. Fahrbach, S. Osterhus, and G. Rohardt (2004), Arctic warming through the Fram Strait: Oceanic heat transport from 3 years of measurements, *J. Geophys. Res.*, 109, C06026, doi:10.1029/2003JC001823.
- Serreze, M. C., J. E. Walsh, F. S. Chapin, T. Osterkamp, M. Dyrgerov, V. Romanovsky, W. C. Oechel, J. Morison, T. Zhang, and R. G. Barry (2000), Observational evidence of recent change in the northern high-latitude environment, *Clim. Change*, 46, 159–207.
- Shackleton, H. J., and N. D. Opdyke (1973), Oxygen isotope and paleomagnetic stratigraphy of equatorial Pacific core V28–238: Oxygen isotope temperatures and ice volume on a 10⁵ year and 10⁶ year scale, *Quat. Res.*, 3, 39–55.
- Shackleton, H. J., J. Imbrie, and M. A. Hall (1983), Oxygen and carbon isotope record of the east Pacific core V19–30: Implications for the formation of deep water in the late Pleistocene North Atlantic, *Earth Planet. Sci. Lett.*, 65, 233–244.
- Solheim, A., and C. F. Forsberg (1996), Norwegian Polar Institute's cruise to the northern margin of Svalbard and the Barents Sea 25/7–2/9, 1994: Marine geology/geophysics and physical oceanography, *Rep. Ser.*, 92, *Nor. Polarinst.*, Oslo.
- Steele, M., and T. Boyd (1998), Retreat of the cold halocline layer in the Arctic Ocean, *J. Geophys. Res.*, 103, 10,419–10,435.
- Steinsund, P. I. (1994), Benthic foraminifera in surface sediments of the Barents and Kara seas: Modern and late Quaternary applications, Ph.D. thesis, 111 pp., Univ. of Tromsø, Tromsø, Norway.
- Stuiver, M., and T. F. Braziunas (1993), Sun, ocean, climate and atmospheric ¹⁴CO₂: An evaluation of casual and spectral relationships, *Holocene*, 3, 289–305.
- Stuiver, M., and P. J. Reimer (1993), Extended ¹⁴C database and revised CALIB radiocarbon calibration program, *Radiocarbon*, 35, 215–230.
- Stuiver, M., P. J. Reimer, E. Bard, J. W. Beck, G. S. Burr, K. A. Haugen, K. A. Kromer, F. G. McCormac, J. van de Plicht, and M. Spurk (1998a), INTCAL98 radiocarbon age calibration 24,000–0 cal BP, *Radiocarbon*, 40, 1041–1083.
- Stuiver, M., P. J. Reimer, and T. F. Braziunas (1998b), High-precision radiocarbon age calibration for terrestrial and marine samples, *Radiocarbon*, 40, 1127–1151.
- Svendsen, J. I., and J. Mangerud (1992), Paleoclimatic inferences from glacial fluctuations on Svalbard during the last 20,000 years, *Clim. Dyn.*, 6, 213–220.
- Svendsen, J. I., and J. Mangerud (1997), Holocene glacial and climatic variations on Spitsbergen, Svalbard, *Holocene*, 7, 45–57.
- Svendsen, J. I., et al. (1999), Maximum extent of the Eurasian ice sheet in the Barents and Kara Sea region during the Weichselian, *Boreas*, 28, 234–241.
- Tarnocai, C. (1999), The effect of climate warming on the carbon balance of crysols in Canada, *Permafrost Periglacial Processes*, 10(3), 251–263.
- Vinje, T. E. (1977), Sea ice conditions in the European sector of the marginal seas of the Arctic, 1966–75, *Aarb. Nor. Polarinst.*, 1975, 163–174.
- Vogt, C., J. Knies, R. F. Spielhagen, and R. Stein (2001), Detailed mineralogical evidence for two nearly identical glacial/deglacial cycles and Atlantic water advection to the Arctic Ocean during the last 90,000 years, *Global Planet. Change*, 31, 23–44.
- Walton, W. R. (1964), Recent foraminiferal ecology and paleoecology, in *Approaches to Paleocology*, edited by J. Imbrie and N. Newell, pp. 151–237, John Wiley, Hoboken, N. J.
- Wollenburg, J. E., and A. Mackensen (1998), Living benthic foraminifera from the central Arctic Ocean: Faunal composition, standing stock and diversity, *Mar. Micropaleontol.*, 34, 153–185.

D. Klitgaard-Kristensen and N. Koç, Norwegian Polar Institute, Polar Environmental Centre, N-9296 Tromsø, Norway.

M. A. Ślubowska, The University Centre in Svalbard, P.O. Box 156, N-9171 Longyearbyen, Norway. (martas@unis.no)

T. L. Rasmussen, Department of Geology, University of Tromsø, Dramsveien 201, N-9037 Tromsø, Norway.

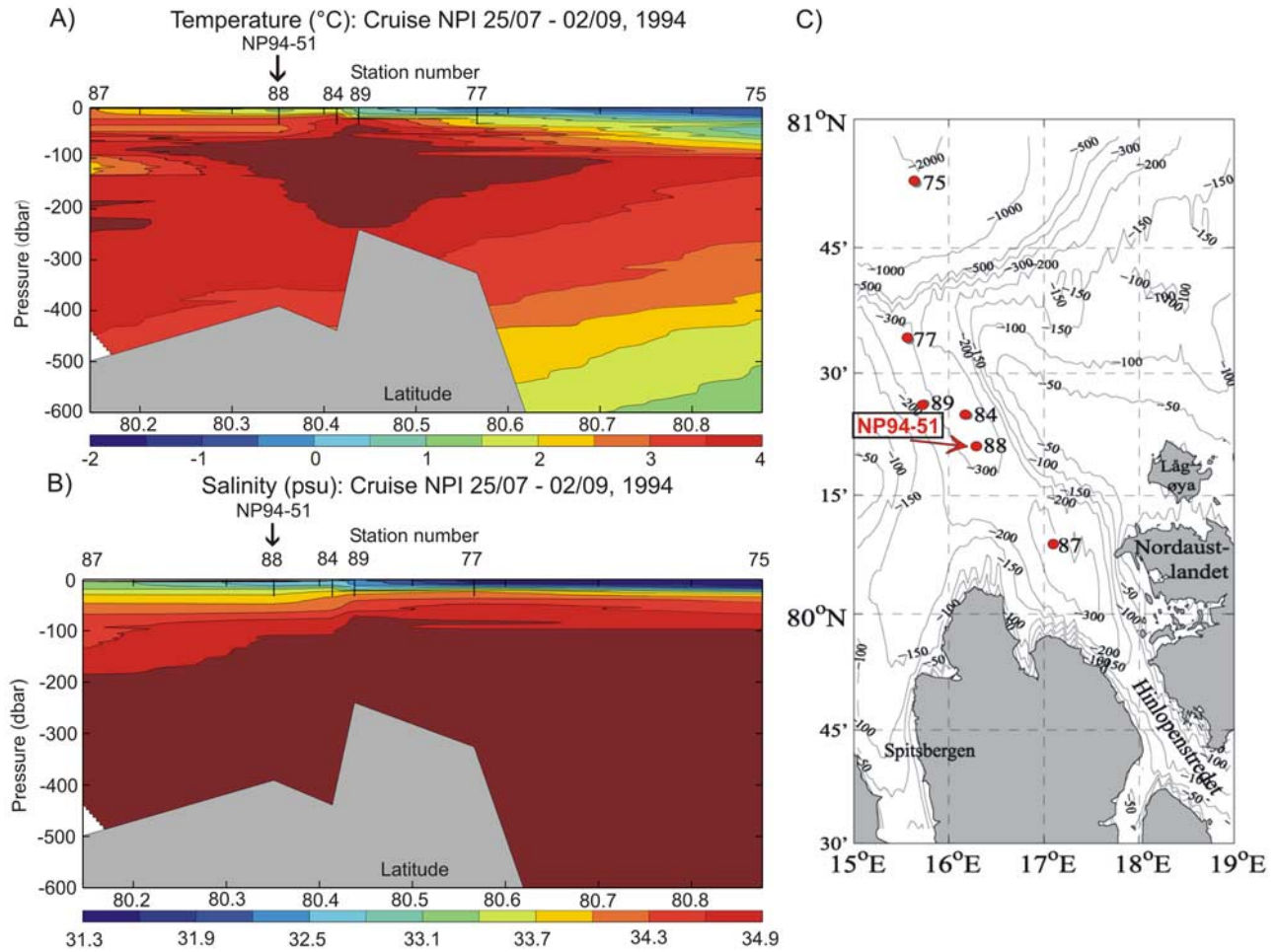


Figure 2. (a) Contours of potential temperature and (b) contours of potential salinity derived from (c) section taken at the northern Svalbard continental margin close to the Hinlopen Strait. Arrow in Figures 2a and 2b indicates the position of the NP94-51 core. The conductivity-temperature-depth (CTD) station measurements, marked by dots on the map (Figure 2c), were taken on 23–29 of August 1994. The sections are shown from S to N, and contour intervals are 1°C for temperature (Figure 2a) and 0.6‰ for salinity (Figure 2b). The CTD station 88 (Figure 2c) was taken at the same location as the NP94-51 core (80°21.40N and 16°17.60E).